International Journal of Mass Spectrometry and Ion Physics, 26 (1978) 327—343

PROTON-TRANSFER REACTIONS IN NITROMETHANE AT 297 K *

GERVASE I. MACKAY and DIETHARD K. BOHME

Department of Chemistry and Centre for Research in Experimental Space Science, York University, Downsview, Ontario M3J 1P3 (Canada)

(Received 16 August 1977)

ABSTRACT

Rate constants for proton-transfer reactions of the type $XH^+ + CH_3NO_2 \rightarrow CH_3NO_2H^+ + X$ (1) where X = H_2, D_2, N_2, CO_2, CH_4, N_2O, CO, H_2O, HCN, CH_3CHCH_2, and CH_3OH, and of the type $CH_3NO_2 + X^- \rightarrow XH + CH_2NO_2^-$ (2) where X = NH_2, H, D, OH, CH_3O, C_2H_5O, C_2H, CH_3COCH_2, and CH_3S have been measured at 297 ± 2 K using the flowing afterglow technique with values ranging from 0.1 to 1.3 × 10^{-8} cm^3 $molecule^{-1}$ s^{-1}. Rate constant and equilibrium ion concentration measurements for proton transfer from $C_3H_7^+$ to CH_3NO_2, from $CH_3NO_2H^+$ to CH_3OH, and from CH_3NO_2 to CH_3S^- provided values for equilibrium constants of 3 ± 1, 1.3 ± 0.4 and 1.9 ± 0.3, respectively, from which values for $PA_{298}(CH_3NO_2) = PA_{298}(CH_3OH) = 181 \pm 3$ kcal mol^{-1} and $PA_{298}(CH_2NO_2^-) = 357.6 \pm 2.8$ kcal mol^{-1} were deduced. Several of the more exothermic members of reactions of type (1) appeared to proceed, at least in part, by dissociative proton transfer to produce NO^+ and CH_3NO^+. In the case of reactions of type (2), proton transfer predominated over exothermic NO_2^- displacement. The measured rate constants are compared with the predictions of the Langevin, average-dipole-orientation and locked-dipole theories of ion—molecule collisions. The average-dipole-orientation theory provides the most realistic collision rates for these reactions although these appear to be underestimated on average by ca. 10% and ca. 5% for reactions of type (1) and (2), respectively. The observed variations of reaction efficiency with exothermicity are discussed in terms of current models of the mechanism for proton transfer.

INTRODUCTION

Extensive rate measurements have been made in our flowing afterglow laboratory during the past few years for a large number of exothermic reactions involving the transfer of a proton either from an ion to a molecule

$$XH^+ + Y \rightarrow YH^+ + X \quad (1)$$

or from a molecule to an ion

$$YH + X^- \rightarrow XH + Y^- \quad (2)$$

* This work was supported by the National Research Council of Canada.

For such reactions involving simple molecular systems in which Y and YH are polar molecules, these measurements have indicated large room-temperature rate constants spanning a range in values from 0.1 to 1.5×10^{-8} cm^3 $molecule^{-1}$ s^{-1} which can generally be accounted for, within experimental error, by the average-dipole-orientation (ADO) collision theory when proton transfer is assumed to proceed on every encounter [1—3]. However, some of these measurements, measurements of momentum-transfer collision frequencies [4], and other theoretical approaches [5] have indicated that the ADO theory, in its present form, may actually underestimate the collision rate. The assumption of unit probability for proton transfer has also come into question [6], especially for more complex molecular systems involving charge-delocalized ions [7]. Attention has been drawn to a number of shortcomings of the ADO collision model, which continues to be extended and refined [8]. Theoretical aspects of proton-transfer reaction probability have largely remained obscure, although valuable qualitative models are beginning to be developed [7]. To provide further experimental insight and support data for future developments in proton-transfer collision and reaction theories, we report here rate and equilibrium-constant measurements for reactions of types (1) and (2) with CH_3NO_2, a highly polar molecule (μ_D = 3.46 D) with a large polarizability (α = 5.2 Å^3). The relatively high proton affinity of CH_3NO_2 and low proton affinity of $CH_2NO_2^-$ allowed the choice of a wide variety of XH^+ ions with X = H_2, D_2, N_2, CO_2, CH_4, N_2O, CO, H_2O, HCN, C_3H_6, and CH_3OH, as well as X^- ions with X = NH_2, H, D, OH, CH_3O, C_2H_5O, C_2H, CH_3COCH_2, and CH_3S.

EXPERIMENTAL

The experiments were carried out in a flowing plasma mass-spectrometer (flowing afterglow) system in the usual manner [9]. Positive ions XH^+, where X = N_2, CO_2, CH_4, N_2O, CO, H_2O, HCN, CH_3CHCH_2, and CH_3OH, were generated according to the proton-transfer reaction

$$H_3^+ + X \rightarrow XH^+ + H_2 \qquad (3)$$

by introducing the appropriate gas, X, upstream of the reaction region into a pure hydrogen afterglow in which H_3^+ is the dominant ion. D_3^+ was established by the fast reaction

$$D_2^+ + D_2 \rightarrow D_3^+ + D \qquad (4)$$

upon the addition of D_2 into a helium plasma. The negative ions were generated in both helium and hydrogen carrier gas either by electron impact on the appropriate neutral reagent — H^-, NH_2^- (NH_3), OH^- (H_2O), CH_3O^- (CH_3OH), $C_2H_5O^-$ (C_2H_5OH) — or by proton transfer to OH^- from C_2H_2, CH_3COCH_3, CH_3SH, and CH_3NO_2 according to the reaction

$$YH + OH^- \rightarrow H_2O + Y^- \qquad (5)$$

The D^- ion was produced by the proton-transfer reaction of NH_2^- with D_2 in a helium plasma only. Typical operating conditions in these experiments encompassed total gas pressures, P, in the range 0.29—0.514 Torr, gas velocities, $\bar{v}$, in the range 7.2—8.1 × 10^3 cm s^{-1}, and reaction lengths, L, of 60 and 85 cm. At the end of the reaction region the plasma was sampled with a quadrupole mass spectrometer through a small orifice mounted at the tip of a sampling nose cone. The observed variations in the reactant and product ion signals as a function of reactant gas addition at a fixed addition of backreactant gas provided the raw data from which the rate and equilibrium constants were derived.

The gases used were helium (Linde, Prepurified Grade, 99.995% He), hydrogen (Linde, Very Dry Grade, 99.95% H_2), deuterium (Matheson, C.P. Grade, 99.5% (atom)), nitrogen (Matheson, Prepurified Grade, 99.998% N_2), carbon monoxide (Matheson, C.P. Grade, 99.5% CO), carbon dioxide (Matheson, Coleman Grade, 99.99% CO_2), nitrous oxide (Matheson, 98.0% N_2O), methane (Matheson, Ultra High Purity, 99.9% CH_4), propene (Matheson C.P. Grade, 99.0% C_3H_6 (liquid phase)), ammonia (Matheson, anhydrous, 99.99% NH_3), boiled distilled water, methanol (BDH, Analytical Reagent), ethanol (Consolidated Chemicals, Absolute, 10% mixture of C_2H_5OH vapour in He), acetylene (Matheson, Prepurified Grade, 99.6% C_2H_2), nitromethane (Fisher Scientific Company, Spectranalyzed Grade, 10% mixture of CH_3NO_2 in He). The HCN was prepared by the action of sulphuric acid on an aqueous solution of KCN [10], dried by passing it over anhydrous $CaCl_2$, and further purified by distillation in vacuo.

RESULTS AND DISCUSSION

The proton affinity of nitromethane

Several years ago Kriemler and Butrill [11] reported the observation in their ion cyclotron resonance spectrometer of a number of proton-transfer reactions involving nitromethane. Negative double resonance signals were recorded for the transfer of a proton from H_3S^+, $C_3H_7^+$, and $CH_3OH_2^+$ to CH_3NO_2, and from $CH_3NO_2H^+$ to CH_3COCH_3, CH_3CHO, and CH_3OH. These observations established the order of proton affinities H_2S, $CH_3CHCH_2 < CH_3OH \simeq CH_3NO_2 < CH_3CHO$, CH_3COCH_3 and led to an estimated value for $PA(CH_3NO_2)$ of ca. 180 kcal mol^{-1} when reference was made to proton affinities available at that time. When reference is made to the proton affinities recently reported by Yamdagni and Kebarle [12], this order leads to a value for $PA(CH_3NO_2)$ of ca. 182 kcal mol^{-1}. With this order as a guide and in an attempt to establish the accuracy of these estimates of $PA(CH_3NO_2)$, we have reinvestigated the proton-transfer reactions

$$C_3H_7^+ + CH_3NO_2 \rightleftharpoons CH_3NO_2H^+ + C_3H_6 \quad (6)$$

$$CH_3NO_2H^+ + CH_3OH \rightleftharpoons CH_3OH_2^+ + CH_3NO_2 \quad (7)$$

Both directions of each reaction were studied in separate experiments. Pro-

ton transfer was observed to be rapid in each case with $k_6 = (2.3 \pm 0.8) \times 10^{-9}$, $k_{-6} = (9.6 \pm 2.4) \times 10^{-10}$, $k_7 = (1.7 \pm 0.4) \times 10^{-9}$, and $k_{-7} = (1.3 \pm 0.3) \times 10^{-10}$ cm^3 molecule^{-1} s^{-1}. These results are all consistent with the earlier qualitative studies of Kriemler and Butrill [11] and provide values for $K_6 = 3 \pm 1$, and $K_7 = 1.3 \pm 0.4$ at 297 ± 2 K.

The equilibrium constant for reaction (6) establishes that $PA_{298}(CH_3NO_2) - PA_{298}(C_3H_6) = 0.6 \pm 0.2$ kcal mol^{-1} with the assumption that $\Delta G^0_{298} = \Delta H^0_{298}$ that $PA_{298}(CH_3NO_2) = 181 \pm 3$ kcal mol^{-1} when the proton affinity of propene is used as a reference. $PA_{298}(CH_3CHCH_2)$ can be derived to be 180 ± 2 kcal mol^{-1} from $\Delta H^0_{f,298}(CH_3CHCH_2) = 4.88 \pm 0.1$ kcal mol^{-1} [13], $\Delta H^0_{f,298}(H^+) = 367.12 \pm 0.01$ kcal mol^{-1} [14] and $\Delta H^0_{f,298}(s\text{-}C_3H_7^+) = 192 \pm 2$ kcal mol^{-1} as reported by Lossing and Semeluk [15]. The difference, $PA_{298}(CH_3OH) - PA_{298}(CH_3NO_2)$ is only 0.16 ± 0.05 kcal mol^{-1} according to the value measured for K_7 and with the assumption that $\Delta G^0_{298} = \Delta H^0_{298}$, so that $PA_{298}(CH_3OH) = 181 \pm 3$ kcal mol^{-1}, which agrees, within experimental error, with previous determinations [16]. Also $PA_{298}(CH_3OH) - PA_{298}(CH_3CHCH_2) = 0.8$ kcal mol^{-1}, which compares favourably with the value of 1.1 kcal mol^{-1} determined recently by Yamdagni and Kebarle [12] from equilibrium constant measurements made with their pulsed electron beam high-pressure ion source mass spectrometer.

Kinetics of reactions of XH^+ with nitromethane

The rate constants for reactions of type (1) were measured from the decay of XH^+ in the usual manner and are summarized in Table 1. The behaviour of positive ions observed upon the addition of CH_3NO_2 into a pure H_2 plasma is shown in Fig. 1. At least three channels appeared to be available for the reaction of H_3^+ with CH_3NO_2:

$$H_3^+ + CH_3NO_2 \rightarrow CH_3NO_2H^+ + H_2 \quad (8a)$$
$$\rightarrow NO^+ + (CH_3OH + H_2) \quad (8b)$$
$$\rightarrow CH_3NO^+ + (OH + H_2) \quad (8c)$$

The choice of the combination of neutral products for channels (8b) and (8c) reflects the dissociative proton-transfer model which will be invoked below to account for the observations made for these reactions. CH_3NO^+ reacts further with CH_3NO_2, apparently by proton and methyl-cation transfer [11] according to

$$CH_3NO^+ + CH_3NO_2 \rightarrow CH_3NO_2H^+ + CH_2NO \quad (9a)$$
$$\rightarrow C_2H_6NO_2^+ + NO \quad (9b)$$

Notwithstanding the uncertainties introduced by this further reaction of CH_3NO^+ and mass discrimination, we estimated branching ratios for reaction (8) of $CH_3NO_2H^+$ (55%), NO^+ (44%), and CH_3NO^+ (1%). Similar observations were recorded for the reaction of D_3^+ with CH_3NO_2. Channel (8b) was also observed for the reactions with N_2H^+, CO_2H^+, CH_5^+, N_2OH^+, and H_3O^+ but in considerably diminished amounts — viz. approximately 0.5, 0.3, 0.07, 0.06,

TABLE 1

Rate constants at 297 ± 2 K (in units of 10^{-9} cm^3 molecule^{-1} s^{-1}) for reactions of the type $XH^+ + CH_3NO_2 \rightarrow CH_3NO_2H^+ + X$

XH^+	k_{exp} [a]	k_{ADO} [b]	k_{exp}/k_{ADO}	$-\Delta H^0_{298}$ [c] (kcal mol^{-1})
H_3^+	8.03 ± 0.10 [4]	7.74	1.04	80 ± 4
D_3^+	5.8 ± 0.6 [3]	5.60	1.04	80 ± 4
CH_5^+	4.13 ± 0.37 [4]	3.59	1.15	50 ± 5
H_3O^+	4.11 ± 0.24 [4]	3.44	1.19	15 ± 5
H_2CN^+	3.75 ± 0.23 [3]	2.99	1.25	10 ± 5
HCO^+	3.33 ± 0.09 [3]	2.95	1.13	38 ± 4
N_2H^+	3.29 ± 0.12 [3]	2.95	1.12	64 ± 4
$CH_3OH_2^+$	1.32 ± 0.04 [3]	2.83	0.47	−0.16 ± 0.05 [e]
$C_3H_7^+$ [d]	2.3 ± 0.3 [3]	2.60	0.88	0.6 ± 0.2 [e]
CO_2H^+	2.82 ± 0.05 [4]	2.57	1.10	52 ± 5
N_2OH^+	2.70 ± 0.02 [3]	2.57	1.05	43 ± 5

[a] The mean value and the precision of the measurements. The accuracy is estimated to be better than ±25%. The number of measurements is given in brackets.
[b] The collision rate constant calculated using the average-dipole-orientation theory (the $\cos\theta$ model) with $C = 0.243$ [17].
[c] Proton affinities adopted for the determination of ΔH^0_{298} are given in Table 2.
[d] Protonated propene.
[e] Based on the equilibrium constant determined in this study with the assumption that $\Delta G^0_{298} = \Delta H^0_{298}$.

and 0.01%, respectively. The data for the H_3O^+ reaction is shown in Fig. 2. Complications introduced by the ^{13}C isotope prevented a determination of this branching ratio in the case of the HCO^+ reaction. Of the ions above, only N_2H^+ produced a measurable amount of CH_3NO^+, viz. channel (8c), and again in much smaller quantities, viz. ca. 0.01%. Proton transfer was the only observed channel for the reactions of H_2CN^+, $C_3H_7^+$, and $CH_3OH_2^+$ with CH_3NO_2.

These observed trends in the branching ratios are reminiscent of the observations made by Futrell and co-workers [18,19] in their systematic measurements of product distributions for proton-transfer reactions, particularly the reactions of H_3^+, O_2H^+ and various protonated rare gases with CH_4, C_2H_4, and C_2H_6. They report a dependence of the observed product distributions on excess energy in the form of internal energy in the reactant ion and/or overall reaction exothermicity and suggest a general direct mechanism for proton transfer, possibly resembling a stripping process. In terms of this mechanism, excess energy is deposited not only as internal energy of the protonated product but also, to a considerable extent, as relative translational energy of the products. Accordingly, proton transfer will not necessarily be completely dissociative even when the excess energy exceeds that required for

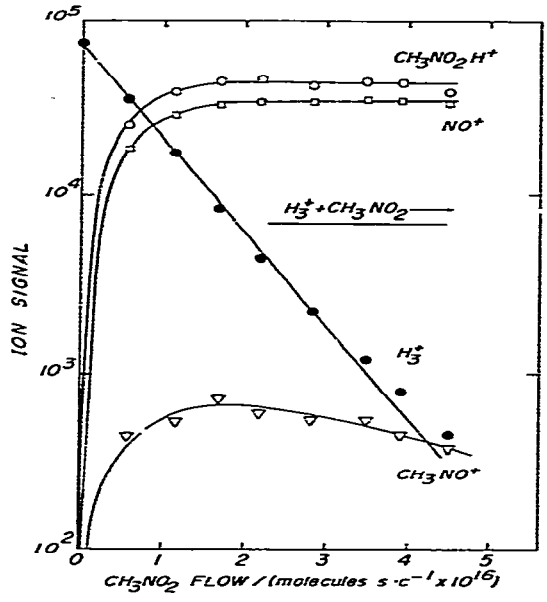

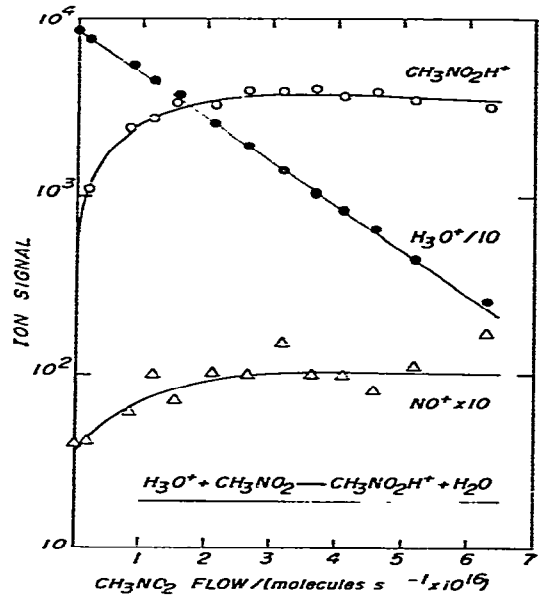

Fig. 1. The variation of major positive ion signals observed upon the addition of CH_3NO_2 into an H_2 plasma in which H_3^+ is initially a dominant ion. The decay of H_3^+ provides a rate constant of 8.0×10^{-9} cm^3 molecule^{-1} s^{-1}. $T = 295$ K, $P = 0.365$ Torr, $\bar{v} = 7.7 \times 10^3$ cm s^{-1}, and $L = 85$ cm.

Fig. 2. The variation of major positive ion signals observed upon the addition of CH_3NO_2 into an H_2O—H_2 plasma in which H_3O^+ is initially a dominant ion. The decay of H_3O^+ provides a rate constant of 4.1×10^{-9} cm^3 molecule^{-1} s^{-1}. $T = 298$ K, $P = 0.400$ Torr, $\bar{v} = 7.7 \times 10^3$ cm s^{-1}, and $L = 85$ cm.

the dissociation of the protonated product.

The minimum excess energy required for the dissociation of $CH_3NO_2H^+$ into NO^+ and CH_3NO^+ is 21 and 32 kcal mol^{-1}, respectively, according to

$$CH_3NO_2H^+ \rightarrow NO^+ + CH_3OH - 21 \text{ kcal mol}^{-1} \quad (10a)$$
$$\rightarrow CH_3NO^+ + OH - 32 \text{ kcal mol}^{-1} \quad (10b)$$

For reactions of type (1) involving relaxed XH^+ ions, this amount of excess energy is available in the form of reaction exothermicity when $PA(X) \leq 161$ and 150 kcal mol^{-1}, respectively. For this calculation the heats of formation of CH_3NO_2 and CH_3NO^+ were taken from the compilation of Franklin et al. [20], those of H^+, OH, and NO^+ from the JANAF Tables [14], and that for CH_3OH from the compilation of Benson et al. [13]. The proton affinities adopted in this work are given in Table 2 from which it is apparent that, of the reactions investigated in this study, those involving HCO^+, N_2OH^+, CH_5^+, CO_2H^+, N_2H^+, and H_3^+ (D_3^+) have the excess energy required for both dissociative proton-transfer channels (increasingly so in that order), whereas the

TABLE 2

Proton affinities (in kcal mol^{-1}) adopted in the determination of ΔH^0_{298}

X	PA_{298}	Ref.	X^-	PA_{298}	Ref.
H_2, D_2	101 ± 1	21	H^-, D^-	400 ± 1	14
N_2	117 ± 1	22	NH_2^-	404 ± 1	25
CO_2	129 ± 2	22	OH^-	391	14
CH_4	131 ± 2	22	CH_3O^-	381 ± 2	26
N_2O	138 ± 2	22	$C_2H_5O^-$	378 ± 3	26
CO	143 ± 1	23	C_2H^-	378 ± 3	26
H_2O	166 ± 2	24	$CH_3COCH_2^-$	366 ± 1	27
HCN	171 ± 2	24	CH_3S^-	357 ± 2	[a]
CH_3CHCH_2	180 ± 2	[a]	$CH_2NO_2^-$	358 ± 3	[a]
CH_3NO_2	181 ± 3	[a]			
CH_3OH	181 ± 3	[a]			

[a] This work, see text.

reactions involving $CH_3OH_2^+$, $C_3H_7^+$, H_2CN^+, and H_3O^+ do not. Although the NO^+ and CH_3NO^+ branching ratios observed in these experiments do not necessarily represent initial product distributions (the extent of collisional stabilization of excited $CH_3NO_2H^+$ at the pressures employed in these experiments is unknown), their trends are consistent with what is expected in terms of this model on the basis of the corresponding excess energies. The reactions of $CH_3OH_2^+$, $C_3H_7^+$, and H_2CN^+ were observed to proceed solely by proton transfer. The ion H_3O^+ appeared to produce trace amounts of NO^+, probably because this channel is only slightly endothermic. For the other ions there was a definite trend in NO^+ production which increased with increasing reaction exothermicity. The CH_3NO^+ ion production was observed only for the very exothermic reactions of N_2H^+ and H_3^+ (D_3^+), again in relatively larger amounts for the more exothermic case. The sum total production of NO^+ and CH_3NO^+ never exceeded ca. 45%, which is qualitatively in agreement with the model mechanism according to which a significant fraction of the excess energy becomes unavailable for internal product-ion excitation as it is partitioned into relative translational energy.

The proton affinity of the nitromethyl anion

Proton abstraction from nitromethane was first investigated by Bohme et al. [28] in their early flowing afterglow studies of gas-phase acidities. These authors reported the observation at 300 K of proton transfer from CH_3NO_2 to n-$C_4H_9S^-$, $C_5H_5^-$, and CCl_3^-, and the gas-phase acidity order n-C_4H_9SH > CH_3NO_2 > C_5H_6 ≥ $CHCl_3$ > CH_3COCH_3. With this order as a guide and in an attempt to provide a quantitative measure for $PA(CH_2NO_2^-)$, we investigated the kinetics and equilibrium for the reaction

$$CH_3S^- + CH_3NO_2 \rightleftharpoons CH_2NO_2^- + CH_3SH \qquad (11)$$

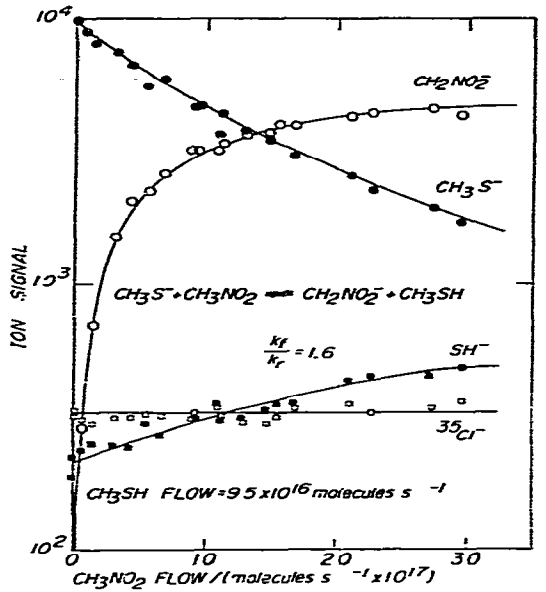

Fig. 3. The observed variation of anion signals upon the addition of CH_3NO_2 into a CH_3SH—H_2O—He plasma in which CH_3S^- is initially a dominant ion. The solid line drawn through the CH_3S^- decay is a fit which provides the values $k_f = 9.0 \times 10^{-10}$ cm^3 molecule^{-1} s^{-1}, $k_r = 5.5 \times 10^{-10}$ cm^3 molecule^{-1} s^{-1}, and $k_f/k_r = 1.6$ for the proton transfer to CH_3S^-. $T = 296$ K, $P = 0.452$ Torr, $\bar{v} = 7.9 \times 10^3$ cm s^{-1}, and $L = 85$ cm.

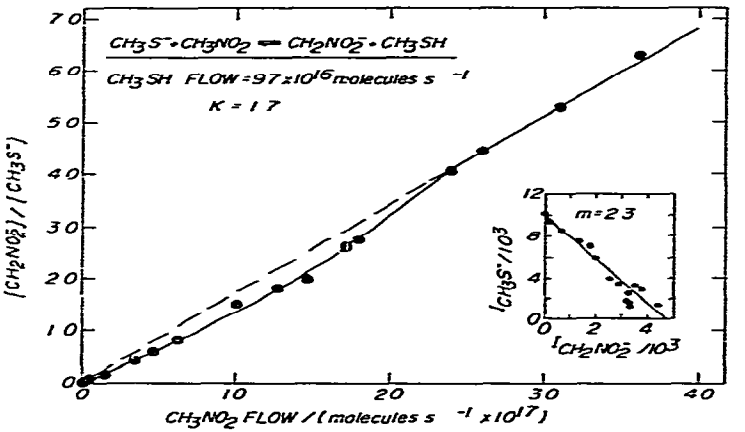

Fig. 4. The observed variation of the product-to-reactant ion signal ratio (corrected for mass discrimination) with the flow of neutral reactant, CH_3NO_2, at constant flow of neutral back-reactant, CH_3SH. The inital curvature represents the approach to equilibrium. K is determined from the slope of the linear region at high CH_3NO_2 flows. The insert illustrates the determination of the mass-discrimination factor, m. $T = 296$ K, $P = 0.452$ Torr, $\bar{v} = 7.9 \times 10^3$ cm s^{-1}, and $L = 85$ cm.

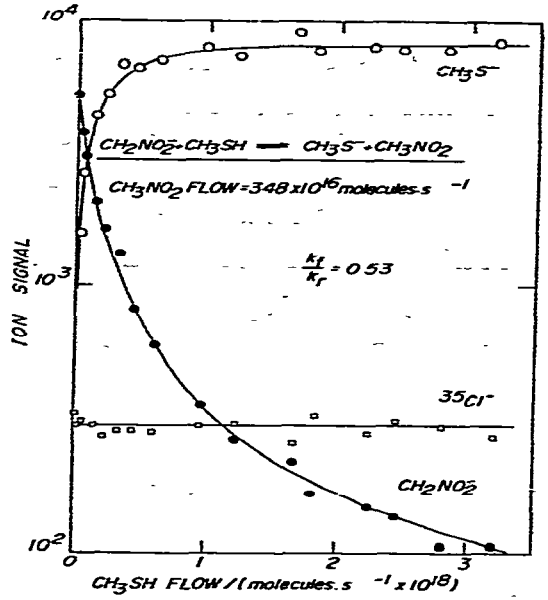

Fig. 5. The observed variation of anion signals upon the addition of CH_3SH into a CH_3NO_2—H_2O—He plasma in which $CH_2NO_2^-$ is initially a dominant ion. The solid line drawn through the decay of $CH_2NO_2^-$ is a fit which provides the values $k_f = 5.0 \times 10^{-10}$ cm^3 molecule^{-1} s^{-1}, $k_r = 9.5 \times 10^{-10}$ cm^3 molecule^{-1} s^{-1}, and $k_f/k_r = 0.53$ for the proton transfer to $CH_2NO_2^-$. T = 296 K, $P = 0.449$ Torr, $\bar{v} = 7.9 \times 10^3$ cm s^{-1}, and $L =$ 85 cm.

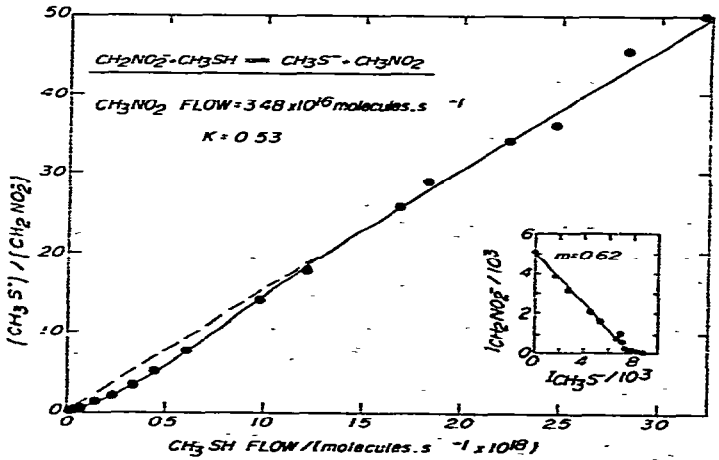

Fig. 6. The observed variation of the product-to-reactant ion signal ratio (corrected for mass discrimination) with the flow of neutral reactant, CH_3SH, at constant flow of neutral back-reactant, CH_3NO_2. The initial curvature represents the approach to equilibrium. K is determined from the slope of the linear region at high CH_3SH flows. The insert illustrates the determination of the mass-discrimination factor, m. $T = 296$ K, $P = 0.449$ Torr, $\bar{v} = 7.9 \times 10^3$ cm s^{-1}, and $L = 85$ cm.

TABLE 3

Summary of the measured values of k_f/k_r and K at 297 ± 2 K for the reaction $CH_3S^- + CH_3NO_2 \rightleftharpoons CH_2NO_2^- + CH_3SH$

Direction studied	N [a]	k_f/k_r [b]	Accuracy	N	K [c]	Accuracy
Forward	3	1.9 ± 0.2 [d]	±30%	3	1.8 ± 0.2	±30%
Reverse	3	1.9 ± 0.1	±25%	3	1.9 ± 0.1	±30%

[a] N represents the number of measurements.
[b] Determined from a fit to the decay of the reactant ion (Analysis B [9]).
[c] Determined from the slope of the ratio plot corrected for mass discrimination (Analysis C [9]).
[d] Best estimate of the precision.

Equilibrium was approached from both directions of reaction (11) as shown in Figs. 3—6. The measured values for k_{11}/k_{-11} and K_{11} are summarized in Table 3 and provided a best estimate of the true value for the equilibrium constant at 297 ± 2 K of 1.9 with a standard error of ±0.3 [29]. The reaction was observed to be rapid in both directions with $k_{11} = (9.4 \pm 2.4) \times 10^{-10}$ and $k_{-11} = (4.9 \pm 1.5) \times 10^{-10}$ cm^3 molecule^{-1} s^{-1}. No serious complications were introduced into the data analysis by competing reaction channels and clustering reactions. There was some evidence for a minor channel (ca. 5%) to the reverse direction of reaction (11), corresponding to the displacement reaction

$$CH_2NO_2^- + CH_3SH \rightarrow SH^- + C_2H_5NO_2 \quad (12)$$

and a slow displacement ($k \lesssim 10^{-12}$ cm^3 molecule^{-1} s^{-1}) of the type

$$CH_3S^- + CH_3SH \rightarrow SH^- + CH_3SCH_3 \quad (13)$$

Both of these reactions are ca. 13 kcal mol^{-1} exothermic.

The equilibrium constant determined for reaction (11) establishes a standard free energy change for this reaction at 298 K of —0.4 ± 0.1 kcal mol^{-1}. The standard entropy change was estimated to be +3 ± 2 e.u. from $S^0(CH_3SH) = 60.96$ e.u. [13], $S^0(CH_3S^-) = S^0(CH_3Cl) = 55.99$ e.u. [14], and $S^0(CH_3NO_2) - S^0(CH_2NO_2^-) = 2 \pm 2$ e.u., which was arrived at from a comparison with similar differences for the acids $CH_3X = CH_3CHO$, CH_3COCH_3, and CH_3CN for which entropies for the isoelectronic neutrals of the corresponding conjugate bases were available [13]. This value for ΔS^0_{298} leads to a value for $\Delta H^0_{298} = PA_{298}(CH_2NO_2^-) - PA(CH_2S^-) = 0.5 \pm 0.7$ kcal mol^{-1} and a value for $PA_{298}(CH_2NO_2^-) = 357.6 \pm 2.8$ kcal mol^{-1} when reference is made to the value of 357.1 ± 2.1 kcal mol^{-1} for $PA_{298}(CH_3S^-)$ which can be derived from $EA_0(CH_3S) = 42.1 \pm 0.9$ kcal mol^{-1} [30] corrected to 298 K, $\Delta H^0_{f,298}(CH_3S) = 28.0 \pm 1.0$ kcal mol^{-1} [31], $\Delta H^0_{f,298}(H^+)$ [14], and $\Delta H^0_{f,298}(CH_3SH) = -5.46 \pm 0.2$ kcal mol^{-1} [13].

The value for $PA_{298}(CH_2NO_2^-)$ derived in this study should refer to protonation at carbon rather than oxygen, a second site of protonation which arises from resonance stabilization in $CH_2NO_2^-$. Protonation in the reverse direction of reaction (11) must occur at the carbon site in our experiments given the large value for k_{-11} and a proton affinity for the oxygen site ca. 6 kcal mol^{-1} lower than that for the carbon site [32].

The value for $PA_{298}(CH_2NO_2^-)$ leads to a value for $\Delta H^0_{f,298}(CH_2NO_2^-) = -27.5 \pm 3.0$ kcal mol^{-1} with $\Delta H^0_{f,298}(CH_3NO_2) = -17.9 \pm 0.2$ kcal mol^{-1} [13] which in turn provides a value for $EA_{298}(CH_2NO_2) = 48 \pm 13$ kcal mol^{-1} with $\Delta H^0_{f,298}(CH_2NO_2) = 20 \pm 10$ kcal mol^{-1} which was estimated assuming a bond strength $D^0_{298}(H—CH_2NO_2) = 90 \pm 10$ kcal mol^{-1} by comparison with other known values for $D^0_{298}(H—CH_2X)$. In separate experiments we have observed the charge-transfer reaction

$$CH_2NO_2^- + NO_2 \rightarrow NO_2^- + CH_2NO_2 \qquad (14)$$

to be rapid, $k_{14} = (6 \pm 2) \times 10^{-10}$ cm^3 molecule^{-1} s^{-1}, which establishes that $EA_{298}(CH_2NO_2^-) \leqslant EA_{298}(NO_2) = 56.4 \pm 1.4$ kcal mol^{-1} [33].

Kinetics of reactions of X^- with nitromethane

The rate constants measured for reactions of X^- with CH_3NO_2 are summarized in Table 4. Their determination from the decay of X^- was straightforward. Figure 7 shows typical results for the reactions of C_2H^- and $CH_3COCH_2^-$. Proton transfer was observed to be the dominant (ca. >95%) reaction channel for all of the reactions investigated. Apparently proton

TABLE 4

Rate constants at 297 ± 2 K (in units of 10^{-9} cm^3 molecule^{-1} s^{-1}) for reactions of the type $X^- + CH_3NO_2 \rightarrow CH_2NO_2^- + XH$

X^-	k_{exp} [a]	k_{ADO} [b]	$\frac{k_{exp}}{k_{ADO}}$	$-\Delta H^0_{298}$ [c] (kcal mol^{-1})
H^-	12.9 ± 0.8 [3]	13.2	0.98	42 ± 4
D^-	9.6 [1]	9.41	1.02	42 ± 4
NH_2^-	4.85 ± 0.46 [3]	3.68	1.32	46 ± 4
OH^-	3.80 ± 0.45 [4]	3.59	1.06	33 ± 3
C_2H^-	2.51 ± 0.16 [3]	3.11	0.81	20 ± 6
CH_3O^-	3.19 ± 0.14 [2]	2.89	1.10	23 ± 5
$C_2H_5O^-$	2.81 ± 0.11 [2]	2.57	1.09	20 ± 6
CH_3S^-	0.94 ± 0.01 [4]	2.54	0.37	−0.5 ± 0.7 [d]
$CH_3COCH_2^-$	1.39 ± 0.11 [3]	2.41	0.58	8 ± 4

[a] The mean value and the precision of the measurements. The accuracy is estimated to be better than ±25%. The number of measurements is given in brackets.

[b] The collision rate constant calculated using the average-dipole-orientation theory (the cos θ model) with $C = 0.243$ [17].

[c] Proton affinities adopted for the determination of ΔH^0_{298} are given in Table 2.

[d] Based on the equilibrium constant determined in this study.

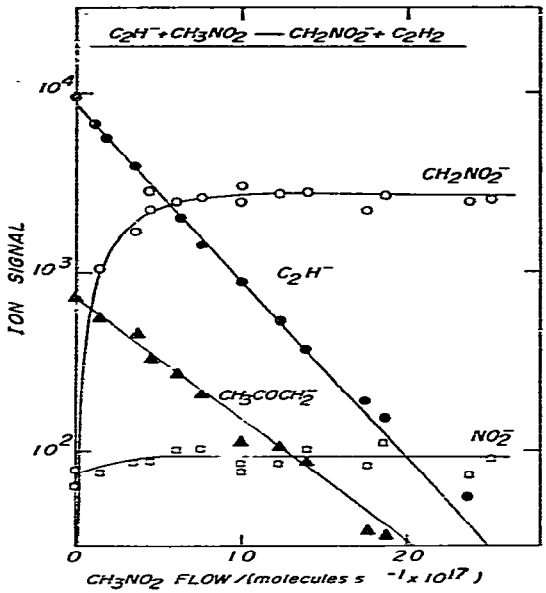

Fig. 7. The variation of major negative ion signals observed upon the addition of CH_3NO_2 into a C_2H_2—H_2O—He plasma in which C_2H^- is initially a dominant ion. The $CH_3COCH_2^-$ arises from the reaction of OH^- and to a lesser extent the reaction of C_2H^- with the acetone impurity in the acetylene. The decays of C_2H^- and $CH_3COCH_2^-$ provide rate constants of 2.4×10^{-9} and 1.3×10^{-9} cm^3 $molecule^{-1}$ s^{-1}, respectively. $T = 296$ K, $P = 0.403$ Torr, $\bar{v} = 7.7 \times 10^3$ cm s^{-1}, and $L = 60$ cm.

transfer dominates at room temperature over nucleophilic displacement of the type

$$X^- + CH_3NO_2 \rightarrow CH_3X + NO_2^- \qquad (15a)$$

which is exothermic for all the anions investigated. The NO_2^- signals monitored at large reagent addition indicated that this channel never exceeded ca. 5%. These results are reminiscent of our previous studies of reactions of anions with CH_3CN for which CN^- displacement also did not compete effectively with proton transfer [34]. Furthermore, there was again no evidence for displacement of the type

$$X^- + CH_3NO_2 \rightarrow X\,CH_2NO_2 + H^- \qquad (15b)$$

This channel is athermal for $X^- = H^-$ and could not be identified in this case since the mass spectrometer cannot distinguish between reactant and product H^- ions. However, the experiments with D^- in which H^- was monitored showed no evidence for its occurrence.

The extent to which the proton transfer is dissociative for these reactions is, of course, unknown since the neutral products are not monitored. Disso-

ciative proton transfer is exothermic for several reactions of X^-, e.g. for the reaction

$$C_2H_5O^- + CH_3NO_2 \rightarrow CH_2NO_2^- + C_2H_5OH \quad (16)$$

sufficient excess energy is available in the form of reaction exothermicity, $\Delta H^0_{298} = -20 \pm 6$ kcal mol^{-1}, to bring about the dissociation of C_2H_5OH into C_2H_4 and H_2O, which requires 11 kcal mol^{-1}.

Comparisons with classical collision theories and exothermicity

Included in Tables 1 and 4 is a comparison of the measured proton-transfer rate constants with the collision rate constants predicted by the ADO theory of Su and Bowers [8,17] according to the expression

$$k_{ADO} = (2\pi q/\mu^{1/2})\,[\alpha^{1/2} + C\mu_D(2/\pi kT)^{1/2}] \quad (17)$$

where q is the charge on the ion, μ is the reduced mass of the reactants, α is the polarizability, and μ_D the permanent dipole moment of the neutral. The "dipole locking constant", C, has been parameterized to have a value between 0 and 1, according to the magnitude of $\mu_D/\alpha^{1/2}$. Expression (17) reduces to the locked-dipole limit, k_{LD}, when $C = 1$ [35,36]. The Langevin expression, k_L, results when $\mu_D = 0$ [37]. All three classical theories define straight lines on a plot of k vs. $\mu^{-1/2}$ for series of homologous reactions of types (1) and (2) for which the neutral substrate remains unchanged. This is illustrated in Fig. 8 in which the measured rate constants for proton transfer with CH_3NO_2 are compared with the collision rate constants predicted by these three theories. The permanent dipole moment for CH_3NO_2, μ_D = 3.46 D, was taken from the compilation of Nelson et al. [38]. The polariza-

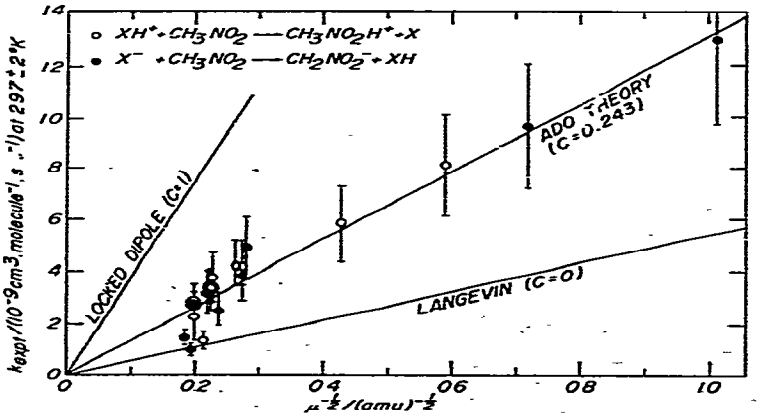

Fig. 8. A comparison of measured rate constants for proton transfer involving nitromethane with capture rate constants predicted by various classical theories of ion–molecule collisions. The solid bars represent the estimated accuracy (±25%) of the measurements which are summarized in Tables 1 and 4.

bility of CH_3NO_2 was estimated to be 5.2 ± 0.3 Å^3 from the bond polarizabilities of C—H and C—N and the NO_2-group polarizability which was estimated from the polarizability of nitrobenzene with the phenyl-group polarizability derived from benzene, toluene, and benzyl chloride [39]. The uncertainty in $\alpha(CH_3NO_2)$ introduces as uncertainty of ca. 2% into the value derived for k_{ADO}.

It is evident from the comparison in Tables 1 and 4 and Fig. 8 that the rate constants determined in this study are most adequately accounted for by the ADO theory, once again reinforcing our general observation that the ADO theory provides the best prediction for proton-transfer reactions involving polar molecules [40]. The ADO theory attributes 58% of the collision rate for these reactions with CH_3NO_2 to ion—permanent dipole interaction. The Langevin theory, which ignores ion—permanent dipole interaction, clearly underestimates the collision rate, whereas the locked-dipole theory appears to overestimate the collision rate.

A closer inspection of the values of k_{exp}/k_{ADO} obtained in this study suggests that the ADO theory may slightly underestimate the collision rate, again in accord with our previous experience. Notwithstanding their experimental uncertainty, the rate constants measured for reactions of type (1) exceed k_{ADO} on average by 10% and as much as 25%, while those measured for the reactions of type (2) exceed k_{ADO} on average by 5% and as much as 32%. The reactions of $CH_3OH_2^+$, CH_3S^- and $CH_3COCH_2^-$ are not included in the averages. The former two reactions are essentially thermoneutral and appear to proceed with a significantly reduced probability of $k_{exp}/k_{ADO} \approx 0.4$. This probability appears to increase sharply as the exothermicity increases, saturating at ca. 1.1 for exothermicities $\gtrsim$10 kcal mol^{-1} (see Fig. 9). Such a trend in reaction probability is consistent with the model invoked by Solka and Harrison [41] to rationalize a similar trend observed by them for reactions of the type

$$CH_3SH_2^+ + Y \rightarrow YH^+ + CH_3SH \qquad (18)$$

for a series of polar molecules, Y, with permanent dipole moments in the range 1.30—2.88 D. According to this model, these reactions can be viewed to proceed through a single proton-bound intermediate of the type $(X...H^+...CH_3NO_2)$ or of the type $(CH_2NO_2^-...H^+...X^-)$ which may decay into reactants or products. Decay into products is increasingly favoured over decay back to reactants as the overall exothermicity of the proton transfer increases. When the two decay channels become energetically identical, i.e. when $PA(X) = PA(CH_3NO_2)$ or when $PA(CH_2NO_2^-) = PA(X^-)$, the reaction rate constant should become equal to $\frac{1}{2}$ the collision rate constant. Farneth and Brauman [7] have recently argued that such a model cannot account for their observations of proton-transfer reactions of type (2) between charge-delocalized anions (enolates, phenoxides, benzyl anion, etc.) and a variety of organic neutrals (ketones, phenols, toluene, etc.). Their pulsed ion cyclotron resonance measurements of rate constants, especially

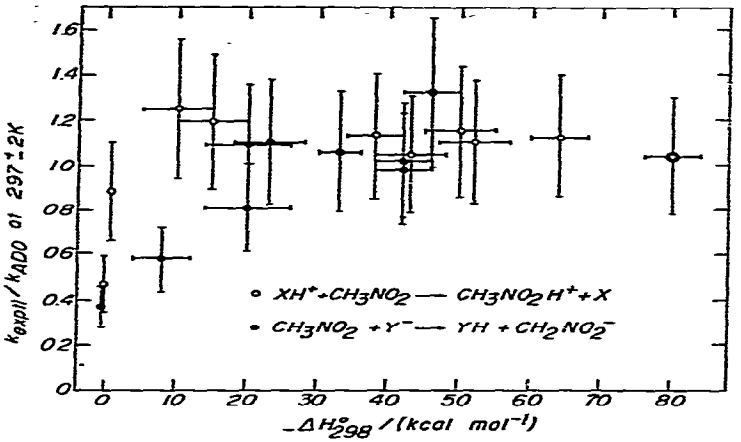

Fig. 9. A plot of the ratio of the measured rate constant for proton transfer with nitromethane to the calculated capture (ADO) rate constant as a function of reaction exothermicity, $-\Delta H^0_{298}$.

for the essentially thermoneutral deuteron-transfer reactions between delocalized anions and their deuterated conjugate acids, e.g.

$$CH_3\overset{O^-}{\overset{|}{C}}=CH_2 + CD_3\overset{O}{\overset{\|}{C}}CD_3 \rightarrow CH_3\overset{O}{\overset{\|}{C}}CH_2D + CD_3\overset{O^-}{\overset{|}{C}}=CD_2 \qquad (19)$$

indicated values in the range 2×10^{-12}—1×10^{-10} cm^3 molecule^{-1} s^{-1}, much lower than $\frac{1}{2}$ the collision rate constant assumed by these authors. They prefer a three-step mechanism according to which the rate of proton transfer is determined by the competitive unimolecular decomposition of a chemically activated intermediate, $(YH...X)^-$, back towards reactants or over a central barrier to products

$$YH + X^- \rightleftharpoons (YH...X)^- \rightleftharpoons (Y...HX)^- \rightleftharpoons Y^- + XH \qquad (20)$$

The central barrier height is the significant rate-determining factor in this model. Farneth and Brauman [7] point out that, within the context of this model, several of their observed trends in rate constants are consistent with enthalpy barriers whose heights are sensitive to overall reaction exothermicity, decreasing as the exothermicity increases. Unfortunately the results reported in this study do not indicate a preference for either model, being qualitatively consistent with both of them. Even the charge-delocalized anion derived by proton removal from acetone was observed to react rapidly with CH_3NO_2, $k = 1.4 \times 10^{-9}$ cm^3 molecule^{-1} s^{-1} with a probability >0.5, in contrast to the observations of Farneth and Brauman [7] who report rate constants of 3.2×10^{-12}, 6.4×10^{-12}, and 3.6×10^{-10} cm^3 mole-

cule^{-1} s^{-1} for the reaction of this anion (or its deuterated analogue) with the more complex organic molecules acetone-d_6, 2-butanone, 3-pentanone, and partially deuterated acetylacetone, respectively.

REFERENCES

1 R.S. Hemsworth, J.D. Payzant, H.I. Schiff and D.K. Bohme, Chem. Phys. Lett., 26 (1974) 417.
2 D. Betowski, J.D. Payzant, G.I. Mackay and D.K. Bohme, Chem. Phys. Lett., 31 (1975) 321.
3 G.I. Mackay, L.D. Betowski, J.D. Payzant, H.I. Schiff and D.K. Bohme, J. Phys. Chem., 80 (1976) 2919.
4 D.P. Ridge and J.L. Beauchamp, Chem. Phys. Lett., 41 (1976) 301.
5 R.A. Barker and D.P. Ridge, J. Chem. Phys., 64 (1976) 4411.
6 E.E. Ferguson, Ann. Rev. Phys. Chem., 26 (1975) 17.
7 W.E. Farneth and J.I. Brauman, J. Am. Chem. Soc., 98 (1976) 7891.
8 M.T. Bowers and T. Su, in P. Ausloos (Ed.), Interactions Between Ions and Molecules, Plenum Press, New York, 1975.
9 D.K. Bohme, R.S. Hemsworth, H.W. Rundle and H.I. Schiff, J. Chem. Phys., 58 (1975) 3504.
10 G. Brauer (Ed.), Handbook of Preparative Inorganic Chemistry, Academic Press, New York, 1965.
11 P. Kriemler and S.E. Buttrill, Jr., J. Am. Chem. Soc., 95 (1973) 1365.
12 R. Yamdagni and P. Kebarle, J. Am. Chem. Soc., 98 (1976) 1320.
13 S.W. Benson, F.R. Cruickshank, D.M. Golden, G.R. Haugen, H.E. O'Neal, A.S. Rodgers, R. Shaw and R. Walsh, Chem. Rev., 69 (1969) 279.
14 JANAF Thermochemical Tables, 2nd edn., Nat. Stand. Ref. Data Ser., Nat. Bur. Stand., (1971) 37. 1974 Supplement, J. Phys. Chem. Ref. Data, (1974) 3.
15 F.P. Lossing and G.P. Semeluk, Can. J. Chem., 48 (1970) 955.
16 J. Long and B. Munson, J. Am. Chem. Soc., 95 (1973) 2427.
17 L. Bass, T. Su, W.J. Chesnavich and M.T. Bowers, Chem. Phys. Lett., 34 (1975) 119.
18 R.D. Smith and J.H. Futrell, Int. J. Mass Spectrom. Ion Phys., 19 (1976) 201; 20 (1976) 43, 71.
19 A. Fiaux, D.L. Smith and J.H. Futrell, Int. J. Mass Spectrom. Ion Phys., 20 (1976) 223.
20 J.L. Franklin, J.G. Dillard, H.M. Rosenstock, J.T. Herron, K. Draxl and F.H. Field, Nat. Stand. Ref. Data Ser., Nat. Bur. Stand., (1969) 26.
21 A.J. Duben and J.P. Lowe, J. Chem. Phys., 55 (1971) 4270.
22 Unpublished results from this laboratory.
23 P.M. Guyon, W.A. Chupka and J. Berkowitz, J. Chem. Phys., 64 (1976) 1419.
24 K. Tanaka, G.I. Mackay and D.K. Bohme, Can. J. Chem., in press.
25 G.I. Mackay, R.S. Hemsworth and D.K. Bohme, Can. J. Chem., 54 (1976) 1624.
26 G.I. Mackay, D.K. Bohme, Can. J. Chem., to be submitted for publication.
27 T.B. McMahon and P. Kebarle, J. Am. Chem. Soc., 98 (1974) 5940.
28 D.K. Bohme, E. Lee-Ruff and L. Brewster Young, J. Am. Chem. Soc., 94 (1972) 5153.
29 N.C. Barford, Experimental Measurements: Precision Error and Truth, Addison-Wesley, London, 1967.
30 K.J. Reed, Ph.D. Thesis, Stanford University, 1975.
31 H.E. O'Neal and S.W. Benson, in J.K. Kochi (Ed.), Free Radicals, Wiley, New York, 1973.
32 P.G. Mezey, A.J. Kresge and I.G. Csizmadia, Can. J. Chem., 54 (1976) 2526.
33 D.B. Dunkin, F.C. Fehsenfeld and E.E. Ferguson, Chem. Phys. Lett., 15 (1972) 257.

34 K. Tanaka, G.I. Mackay, J.D. Payzant and D.K. Bohme, Can. J. Chem., 10 (1976) 1643.
35 T.F. Moran and W.H. Hamill, J. Chem. Phys., 39 (1963) 1413.
36 S.K. Gupta, E.G. Jones, A.G. Harrison and J.T. Myher, Can. J. Chem., 45 (1967) 3107.
37 G. Gioumousis and D.P. Stevenson, J. Chem. Phys., 29 (1958) 294.
38 R.D. Nelson, D.R. Lide and A.A. Manyott, Nat. Stand. Ref. Data Ser., Nat. Bur. Stand., (1967) 10.
39 H. Stuart, in A. Eucken (Ed.), Landolt—Bornstein Zahlenwerte und Funktionen, Vol. I, Section 3, 6th edn., Springer, Berlin, 1951, p. 509.
40 D.K. Bohme, in P. Ausloos (Ed.), Interactions Between Ions and Molecules, Plenum Press, New York, 1975.
41 B.H. Solka and A.G. Harrison, Int. J. Mass Spectrom. Ion Phys., 17 (1975) 379.